Viral Vascular Endothelial Growth Factors Vary Extensively in Amino Acid Sequence, Receptor-binding Specificities, and the Ability to Induce Vascular Permeability yet Are Uniformly...

Article *in* Journal of Biological Chemistry · October 2003

DOI: 10.1074/jbc.M301194200 · Source: PubMed

CITATIONS
70

READS
207

9 authors, including:

Lyn M Wise
University of Otago
48 PUBLICATIONS **2,376** CITATIONS
SEE PROFILE

Norihito Ueda
Daiichi Sankyo
21 PUBLICATIONS **785** CITATIONS
SEE PROFILE

Nicola Dryden
Thermo Fisher Scientific
41 PUBLICATIONS **1,830** CITATIONS
SEE PROFILE

Carol Caesar
Peter MacCallum Cancer Centre
14 PUBLICATIONS **2,619** CITATIONS
SEE PROFILE

THE JOURNAL OF BIOLOGICAL CHEMISTRY
Vol. 278, No. 39, Issue of September 26, pp. 38004–38014, 2003

Printed in U.S.A.

Viral Vascular Endothelial Growth Factors Vary Extensively in Amino Acid Sequence, Receptor-binding Specificities, and the Ability to Induce Vascular Permeability yet Are Uniformly Active Mitogens*

Received for publication, February 4, 2003, and in revised form, June 24, 2003
Published, JBC Papers in Press, July 15, 2003, DOI 10.1074/jbc.M301194200

Lyn M. Wise‡§, Norihito Ueda‡, Nicola H. Dryden‡, Stephen B. Fleming‡, Carol Caesar§, Sally Roufail§, Marc G. Achen§, Steven A. Stacker§¶, and Andrew A. Mercer‡¶‖

From the ‡Virus Research Unit, Department of Microbiology, University of Otago, P.O. Box 56, Dunedin, New Zealand and the §Ludwig Institute for Cancer Research, P.O. Box 2008, Royal Melbourne Hospital, Victoria 3050, Australia

Infections of humans and ungulates by parapoxviruses result in skin lesions characterized by extensive vascular changes that have been linked to viral-encoded homologues of vascular endothelial growth factor (VEGF). VEGF acts via a family of receptors (VEGFRs) to mediate endothelial cell proliferation, vascular permeability, and angiogenesis. The VEGF genes from independent parapoxvirus isolates show an extraordinary degree of inter-strain sequence variation. We conducted functional comparisons of five representatives of the divergent viral VEGFs. These revealed that despite the sequence divergence, all were equally active mitogens, stimulating proliferation of human endothelial cells *in vitro* and vascularization of sheep skin *in vivo* with potencies equivalent to VEGF. This was achieved even though the viral VEGFs bound VEGFR-2 less avidly than did VEGF. Surprisingly the viral VEGFs varied in their ability to cross-link VEGFR-2, induce vascular permeability and bind neuropilin-1. Correlations between these three activities were detected. In addition it was possible to correlate these functional variations with certain sequence and structural motifs specific to the viral VEGFs. In contrast to the conserved ability to bind human VEGFR-2, the viral growth factors did not bind either VEGFR-1 or VEGFR-3. We propose that the extensive sequence divergence seen in the viral VEGFs was generated primarily by selection against VEGFR-1 binding.

Members of the vascular endothelial growth factor (VEGF)[1] family of proteins have emerged as major regulators of the formation of new blood vessels during vasculogenesis and angiogenesis (reviewed in Refs. 1–3). These proteins play critical roles during embryogenesis and in the normal adult, during wound healing and in pathological conditions such as tumor formation. The original member of the family, VEGF-A, also known as vascular permeability factor, was characterized as a mitogen for vascular endothelial cells (4, 5) and a potent inducer of vascular permeability (6). Subsequently, the discovery and characterization of other proteins, related in structure and receptor specificity to VEGF-A have been reported. Currently, the mammalian VEGF family includes VEGF-A, placenta growth factor (PlGF) (7), VEGF-B (8), VEGF-C (9), and VEGF-D (10). VEGF family members are, in general, secreted glycoproteins, which form either disulphide-linked or non-covalent homodimers (5, 7–10). The common structural feature of the VEGF family is the cystine knot motif, which is located in the most highly conserved region of these proteins designated the VEGF homology domain (VHD) (11).

VEGF family members are ligands for a number of mammalian tyrosine kinase receptors: VEGFR-1 (flt-1) (12), VEGFR-2 (flk-1/KDR) (13), and VEGFR-3 (flt-4) (9). It appears that VEGFR-1 plays a role in vascular endothelial cell differentiation and migration, possibly by acting as a ligand-binding molecule, sequestering VEGF-A from VEGFR-2 signaling (14). VEGFR-2 is involved in vascular endothelial cell mitogenesis (13), and VEGFR-3 is involved in the regulation of the lymphatic vasculature (15, 16). VEGFR-1 binds VEGF-A, VEGF-B, and PlGF (12, 17, 18). VEGFR-2 binds VEGF-A, VEGF-C, and VEGF-D (9, 10, 13). VEGFR-3 binds VEGF-C and VEGF-D (9, 10). In addition, the neuronal cell guidance receptors, neuropilin-1 (NP-1) and neuropilin-2, have recently been discovered to interact with VEGF-A, PlGF, and VEGF-B and are thought to act as co-receptors that enhance binding to the VEGFRs (19–22). The role of the VEGFRs in the induction of vascular permeability is, however, unclear.

We and others (21, 23–27) have recently reported a group of poxvirus-derived VEGF-like factors. These proteins have significant homology to VEGF-A and are encoded by *Orf virus* and *Pseudocowpox virus*. *Orf virus* and *Pseudocowpox virus* are distinct species within the genus *Parapoxvirus*, and infect sheep and goats and cattle, respectively, but both readily infect humans (28, 29). The resulting lesions in the skin demonstrate extensive vascular dilation, dermal edema, and proliferation of

* This work was supported in part by funding from the Health Research Council of New Zealand, National Health and Medical Research Council of Australia, Pharmacia Foundation, Australia, and the Cancer Council of Victoria. The costs of publication of this article were defrayed in part by the payment of page charges. This article must therefore be hereby marked "*advertisement*" in accordance with 18 U.S.C. Section 1734 solely to indicate this fact.

¶ These authors contributed equally to this study.

‖ To whom correspondence and reprint requests should be addressed. Tel.: 64-3-4797730; Fax: 64-3-4797744; E-mail: andy.mercer@stonebow.otago.ac.nz.

[1] The abbreviations used are: VEGF, vascular endothelial growth factor; VEGFR, vascular endothelial growth factor receptor; VHD, VEGF homology domain; hVEGF-DΔNΔC, human VEGF-D VHD; $mVEGF_{164}$, mouse VEGF isoform 164; $ORFV_{NZ10}$VEGF, VEGF from *Orf virus* strain NZ10; $ORFV_{NZ2}$VEGF, VEGF from *Orf virus* strain NZ2; $ORFV_{NZ7}$VEGF, VEGF from *Orf virus* strain NZ7; $ORFV_{D1701}$VEGF, VEGF from *Orf virus* strain D1701; $PCPV_{VR634}$VEGF, VEGF from *Pseudocowpox virus* strain VR634; BSA, bovine serum albumin; HMVEC, human microvascular endothelial cells; IL, interleukin; NP-1, neuropilin-1; PlGF, placenta growth factor; PBS, phosphate-buffered saline; ELISA, enzyme-linked immunosorbent assay; NR, non-reducing; R, reducing.

endothelial cells (28, 30). We have shown that the disruption of the VEGF-like gene in *Orf virus* strain NZ2 markedly reduces these characteristics of infection (31). Comparisons of the VEGF-like genes from 24 isolates of *Orf virus* have revealed a surprising degree of sequence variation between isolates (26). The majority of VEGF-like genes were similar to that of *Orf virus* strain NZ2. Although these could be grouped as NZ2-like VEGFs, they showed levels of amino acid identity (average between isolates of 86.1%) more reminiscent of that seen between species of poxviruses than inter-strain variation. A few isolates carried genes identical or very nearly identical to the VEGF-like gene from *Orf virus* strain NZ7, which shares only 43.6% amino acid identity with the VEGF encoded by strain NZ2 ($ORFV_{NZ2}$VEGF). The VEGF from another species of parapoxvirus, *Pseudocowpox virus*, strain VR634, shares only 41.4 and 60.8% amino acid identity with $ORFV_{NZ2}$VEGF and $ORFV_{NZ7}$VEGF, respectively (27).

The extent of sequence variation seen between members of the viral subfamily raises the possibility that these sequence differences might give rise to functional variations. We and others reported previously that the VEGFs from *Orf virus* strains NZ2, NZ7, and D1701 and that from *Pseudocowpox virus* strain VR634 share some of the properties of mammalian VEGF (21, 24, 25, 27). However, the viral VEGFs differ from the cellular family members in their distinct receptor binding profile recognizing VEGFR-2 but not VEGFR-1 or VEGFR-3. In addition, the VEGF from *Orf virus* strain NZ2 has been shown to bind NP-1 (21). The functional studies to date have each examined only a single viral VEGF and differences in the protein expression and assay systems used in the different studies make direct comparisons difficult. In this study we quantitatively compared five of the more divergent variants of the viral VEGFs to determine whether this variation in sequence translates to quantitative differences in receptor-binding specificity and biological activity.

EXPERIMENTAL PROCEDURES

Cloning—DNA fragments containing nucleotides 4–398, 4–398, and 4–406 of the VEGF-like genes of *Orf virus* strains NZ10, D1701, and NZ7, respectively, were prepared by PCR using viral DNA as the templates (23, 26). These fragments were inserted into the pEFBOS-I-FLAG expression vector (C. MacFarlane, Walter and Eliza Hall Institute, Melbourne) (32) immediately upstream from the DNA sequence encoding the FLAG octapeptide (Scientific Imaging Systems). The proteins derived from *Orf virus* strains NZ2, NZ10, D1701, and NZ7 were designated $ORFV_{NZ2}$VEGF, $ORFV_{NZ10}$VEGF, $ORFV_{D1701}$VEGF, and $ORFV_{NZ7}$VEGF, respectively. Also available were equivalent vectors, containing nucleotides 4–401 from *Orf virus* strain NZ2 (21), nucleotides 4–458 from *Pseudocowpox virus* strain VR634 (27), and nucleotides 4–576 of mouse $VEGF_{164}$ (33). *Xba*I fragments from the vectors described above, containing the VEGF coding regions and FLAG octapeptide, were subcloned into the mammalian expression vector, pAPEX-3 (34). Protein synthesis from these vectors would therefore give rise to secreted polypeptides that were tagged with the FLAG octapeptide at their C termini. The proteins derived from *Pseudocowpox virus* and mouse VEGF, were designated $PCPV_{VR634}$VEGF and $mVEGF_{164}$, respectively. An equivalent vector, pVDAPEXΔNΔC, containing amino acids 93–201 from human VEGF-D (10) expresses a truncated secreted VEGF-D polypeptide with the FLAG octapeptide at its N terminus. This protein was designated hVEGF-DΔNΔC.

Expression and Purification—FLAG-tagged proteins were expressed by transfection of 293EBNA cells, with pAPEX-3 vectors with or without VEGF inserts, using FuGENE 6 (Roche Diagnostics), and the proteins were purified by affinity chromatography with M2 (anti-FLAG, Sigma) monoclonal antibody as previously described (21). A mock elution sample was obtained from conditioned medium from pAPEX-3 transfected 293EBNA cells that underwent an identical purification process to the FLAG-tagged proteins.

Analysis and Quantification—Purified proteins were combined with SDS-PAGE sample buffer either with or without 2% 2-mercaptoethanol, boiled, and resolved by SDS-PAGE. When required proteins were transferred to nitrocellulose and visualized by detection with an M2 (anti-FLAG) antibody as described elsewhere (21).

Serial dilutions of control proteins of known concentration (carbonic anhydrase, BSA, and VEGF-DΔNΔC), and the purified VEGF proteins were resolved by SDS-PAGE. The proteins were then stained with Coomassie blue, and the bands were quantitated using a densitometer and the Quantity One program (Bio-Rad Laboratories). A standard curve obtained for the control protein was used to determine the amount of purified VEGF protein present in each sample.

Construction of VEGFR-2-Ig Fusion Proteins—DNA fragments containing the coding region for the first four Ig-like domains of human and mouse VEGFR-2 were amplified by PCR from the templates Signal pIgplus-KDR (Y. Gunji, Haartman Institute, Helsinki, Finland) (10, 21) and VEGFR2-EX-FLAG (33), respectively. The DNA fragments were then cloned into the expression vector pAPEX-Fc-FLAG (M. Halford, Ludwig Institute of Cancer Research, Melbourne, Australia) immediately upstream from DNA sequences encoding the Fc portion of human IgG1 and the FLAG octapeptide. Protein synthesis would, therefore, give rise to secreted FLAG-tagged VEGFR-2-Ig fusion proteins.

Mitogenic Assay with Human Microvascular Endothelial Cells—Human microvascular endothelial cells (HMVEC) were seeded at 10^4 cells per well into a 24-well plate and were allowed to adhere. Samples of purified growth factors were serially diluted in medium with reduced serum and without growth supplements. Cells were then incubated in the media for 72 h at 37 °C, and proliferation was measured by direct counting.

Miles Assay for Vascular Permeability—The Miles vascular permeability assay was performed using anesthetized guinea pigs as previously described (35). Animals were given an intracardiac injection of 500 μl of 0.5% Evans blue dye in PBS to introduce the dye into the blood stream. Samples of purified growth factors were diluted in PBS and 100 μl was injected intradermally into a shaved area on the back of each animal. After 30 min, animals were sacrificed and an area of skin excised. The dye was then eluted from the skin sample in formamide and quantitated by measuring the OD at 620 nm. Controls of 20 ng/ml VEGF and PBS alone were also administered to each animal to allow normalization across animals.

In Vivo Assay in Sheep Skin—Each of the purified proteins were diluted to 20 ng/μl in PBS, 100 μl of which was injected intradermally at duplicate sites within the wool-free regions of the inside hind legs of two sheep. Animals were divided into three groups of two and each group was given duplicate injections of either $ORFV_{NZ2}$VEGF, $ORFV_{NZ10}$VEGF, and $ORFV_{D1701}$VEGF, or $ORFV_{NZ7}$VEGF, $PCPV_{VR634}$-VEGF, and hVEGF-DΔNΔC, or the control samples, FLAG-tagged ovine IL-10, *Orf virus* IL-10, and a mock purification sample. PBS and $mVEGF_{164}$ were also administered to each hind leg of individual animals to allow comparison between groups. Boost injections of identical samples were administered to each site after 72 h. 4 mm biopsies were taken from each site and adjacent areas of untreated skin after 9 days. Biopsies were fixed in 10% neutral buffered formalin and processed into paraffin wax. Two 4 μm, serial sections were taken ~100 μm into the biopsy within the fixed block, followed by two more serial sections, each 100 μm apart. Paired sections were then stained with hematoxylin and eosin or used for immunohistochemical analysis of vascularization. Vascular endothelial cells were identified using a polyclonal rabbit anti-human von Willebrand factor antiserum (Dako). To quantitate the extent of dermal vascularization, four grids covering a combined area of 0.2 mm^2 were overlaid on areas of dermis, avoiding glands and hair follicles. The side of each grid measured 0.224 mm and was divided by 10 equidistant lines. The points at which stained endothelial cells crossed the intersecting points of the grids were counted, and the areal fraction of vascularized dermis was expressed as the fraction of the intersecting points on which stained cells fell. The average areal fraction of vascularization was determined from three semi-serial sections per inoculation site and from four equivalent samples from different animals.

Binding Assays with Soluble VEGFR Extracellular Domains—VEGFR-3-Ig (K. Pajusola, Haartman Institute, Helsinki, Finland) and FLAG-tagged VEGFR-2-Ig fusion proteins were expressed in 293EBNA cells. Cells were incubated for 24 h after transfection then serum-starved for 24 h in Dulbecco's modified Eagle's medium containing 0.2% BSA. The fusion proteins were precipitated from the clarified conditioned medium using protein A-Sepharose beads. Purified VEGFR-1-Ig fusion protein (R&D Systems) was also precipitated using protein A-Sepharose beads. 900 μl of conditioned medium from 293EBNA cells that had been transfected with expression plasmids encoding one of the growth factors or a vector control and then biosynthetically labeled with [^{35}S]Cys for 6 h were combined with 100 μl of 10 X Binding Buffer (5% BSA, 0.2% Tween 20, and 10 μg/ml heparin (VEGFR-2 only)) and either

anti-FLAG (M2) or VEGFR-Ig fusion protein-bound beads. After 3 h at room temperature, the Sepharose beads were washed three times with binding buffer at 4 °C. Bound proteins were released by boiling in SDS-PAGE sample buffer and resolved by SDS-PAGE under reducing conditions. Radiolabelled proteins were detected by a phosphorimaging analyzer (Molecular Dynamics) and were quantitated using the program Quantity One (Bio-Rad Laboratories). Levels of binding to the Ig fusion proteins were quantitated and expressed as a relative binding index, a ratio of the amount of labeled protein precipitated by each receptor, compared with that precipitated by anti-FLAG beads alone.

Bioassays for the Binding and Cross-linking of the Extracellular Domains of VEGFR-2 and VEGFR-3—Bioassays for monitoring the binding and cross-linking of VEGFR-2 and VEGFR-3 involved the use of cell lines expressing chimeric receptors consisting of the extracellular, ligand-binding domains of mouse VEGFR-2 or human VEGFR-3 and the transmembrane and cytoplasmic domains of the erythropoietin receptor (33, 36). The chimeric receptors are expressed by a Ba/F3-derived cell line that survives and proliferates in the presence of interleukin-3 (IL-3) but which dies after IL-3 deprivation. It has previously been shown that signaling from the cytoplasmic erythropoietin receptor domain of the chimeric receptors upon ligand binding is capable of rescuing these cells in the absence of IL-3, thereby allowing detection of specific ligand binding and cross-linking of the extracellular domains of these receptors (10, 21, 27, 33, 36–38).

Samples of purified growth factors were serially diluted in cell culture medium deficient in IL-3. The bioassay cell lines were then incubated in the supplemented media for 48 h at 37 °C. DNA synthesis was quantitated by including 1 μCi of [^{3}H]thymidine during the final 4 h of incubation followed by harvesting using an automated cell harvester (Tomtec®). Incorporated [^{3}H]thymidine was measured by β-counting (Canberra Packard Top Count NXT^{TM} scintillation counter).

ELISA of Binding to Soluble NP-1 Extracellular Domains—96-well Maxisorp immunoplates (Nunc) were coated with purified rat NP-1-Ig fusion protein (R&D Systems) at 2 μg/ml in PBS at 4 °C for 16 h and then blocked with 0.5% BSA and 0.25% Tween 20 at 37 °C for 1 h. Plates were washed between steps with binding buffer (0.5% BSA, 0.25% Tween 20, and 2 μg/ml heparin (Sigma)). Samples of purified growth factors, serially diluted in binding buffer, were then incubated with the immobilized NP-1 at 37 °C for 2.5 h. Horseradish peroxidase-conjugated M2 (anti-FLAG) antibody (Sigma) was used to detect bound growth factors at 37 °C for 1 h and was developed with o-phenylenediamine substrate (Sigma) and quantitated by measuring the OD at 490 nm.

Statistical Analyses—Statistical analysis of the data obtained from each assay was performed using analysis of variance (single factor analysis of variance) with significant points of difference ($p \leq 0.05$) determined using the Tukey's test. Statistical analysis was also used to determine whether there were significant correlations ($p \leq 0.05$) between the results of the individual assays.

Prediction of the Tertiary Structure of the Viral Variants of VEGF—The structures of the variant viral VEGFs were modeled using SWISS-MODEL and the SWISSPDBVIEWER protein modeling program (version 3.5) (39), which are both available from the ExPASy website (www.expasy.ch/spdbv). The sequences of the variants were aligned using SWISSMODEL against protein subunits A and B of human VEGF-A (40) (Protein Data Bank identifier 2VPF). The Iterative Magic Fit function was used for energy minimization, and the alignments were manually optimized.

RESULTS

Extensive Sequence Variation Among Parapoxvirus VEGFs—Alignment of the predicted amino acid sequence of representatives of the viral VEGF family with the VHD of mouse VEGF-A and human VEGF-D, demonstrates the degree of variation between the viral VEGF variants (42.1–87.7% identity), despite conservation of the cystine knot motif characteristic of this family of proteins (Fig. 1). The variation between each of the viral VEGFs and the mammalian VEGFs used in this study is also evident (25.5–37.3% identity). The VHDs of the mammalian members of the VEGF family, VEGF-A, VEGF-B, VEGF-C, and VEGF-D, share between 34 and 59% amino acid identity, but variation between species within each group is typically very limited (for example, human, mouse, ovine, and bovine VEGF-A share an average amino acid identity of 91%). The degree of variation between the viral and mammalian VEGFs is similar to that within the mammalian VEGF family group.

The extensive sequence variation between the viral VEGFs in conjunction with the known functional differences within the mammalian VEGF family group raises the question of whether this variation between the viral VEGFs also translates to quantitative differences in receptor-binding specificity and biological function.

Expression and Purification of Viral VEGF Variants—Mouse $VEGF_{164}$ and the viral VEGFs, tagged at the C terminus with the FLAG octapeptide, were expressed and purified. Human VEGF-DΔNΔC, which consists of the VHD of VEGF-D, was tagged at the N terminus with the FLAG octapeptide and was similarly expressed and purified. The purified proteins were identified using SDS-PAGE, under non-reducing (NR) and reducing (R) conditions, Coomassie blue staining, and Western blot analysis (data not shown). Bands were observed for $mVEGF_{164}$ (NR ≈ 44–48 kDa, R ≈ 22–26 kDa), hVEGF-DΔNΔC (NR ≈ 20–22 kDa, R ≈ 20–22 kDa), $ORFV_{NZ2}VEGF$ (NR ≈ 46–48 kDa, R ≈ 25–28 kDa), $ORFV_{NZ10}VEGF$ (NR ≈ 46–48 kDa, R ≈ 24–26 kDa), $ORFV_{D1701}VEGF$ (NR ≈ 45–47 kDa, R ≈ 24–28 kDa), $ORFV_{NZ7}VEGF$ (NR ≈ 50–52 kDa, R ≈ 26–27 kDa), and $PCPV_{VR634}VEGF$ (NR ≈ 48–52 kDa, R ≈ 28–30 kDa). The bands detected were consistent with $mVEGF_{164}$, $ORFV_{NZ2}VEGF$, $ORFV_{NZ10}VEGF$, $ORFV_{D1701}VEGF$, $ORFV_{NZ7}VEGF$, and $PCPV_{VR634}VEGF$ being disulphide-linked homodimers. The bands detected for hVEGF-DΔNΔC were consistent with hVEGF-DΔNΔC existing as a non-covalent homodimer as reported previously (33). The observation that the monomeric molecular masses of the viral VEGFs were all larger than their predicted sizes can be attributed to the conservation of potential *N* and *O*-linked glycosylation sites (Fig. 1*A*). Concurrent *N*-glycosidase, sialydase, and *O*-glycosidase treatment has been shown to reduce the monomeric size of $ORFV_{NZ2}VEGF$ and $PCPV_{VR634}VEGF$ to ≈ 17 kDa and ≈ 23 kDa, respectively (21, 27).

Viral VEGF Variants Are Mitogenic for Endothelial Cells—Members of the VEGF family of proteins show different degrees of mitogenicity for endothelial cells. The mitogenic capacity of the viral VEGF variants was tested by exposing HMVECs to the purified factors and assessing cell growth after 3 days. Mouse $VEGF_{164}$ and each of the viral VEGFs were able to stimulate a significant increase ($p \leq 0.05$) in the numbers of cells compared with medium that contained no added growth factors (Fig. 2*A*). Statistical analysis revealed that at the highest concentration tested (500 ng/ml) $mVEGF_{164}$ and $PCPV_{VR634}VEGF$ induced significantly higher levels of cellular proliferation than the orf virus VEGFs. At low concentrations, however, $ORFV_{NZ2}VEGF$ (1 ng/ml) and $ORFV_{NZ7}VEGF$ (0.5 and 1 ng/ml) were significantly more potent than $mVEGF_{164}$. Within the intermediate concentration range (2–125 ng/ml) there were no significant differences in potency between the viral VEGFs or between the viral VEGFs and $mVEGF_{164}$. These results clearly demonstrate that all of the viral VEGF variants are effective mitogens for human endothelial cells.

Viral VEGF Variants Differ in Their Abilities to Induce Vascular Permeability—Members of the VEGF family of proteins show differing abilities to induce vascular permeability. The viral VEGF variants were therefore tested in the Miles assay of vascular permeability. Mouse $VEGF_{164}$ and each of the viral VEGFs were able to induce permeability significant ($p \leq 0.05$) greater than that of PBS alone (Fig. 2*B*). Statistical analysis revealed that all the viral VEGF variants were significantly less potent than $mVEGF_{164}$. At the highest concentration at which they were tested (2000 ng/ml) the viral VEGFs also differed between each other in their abilities to induce vascular

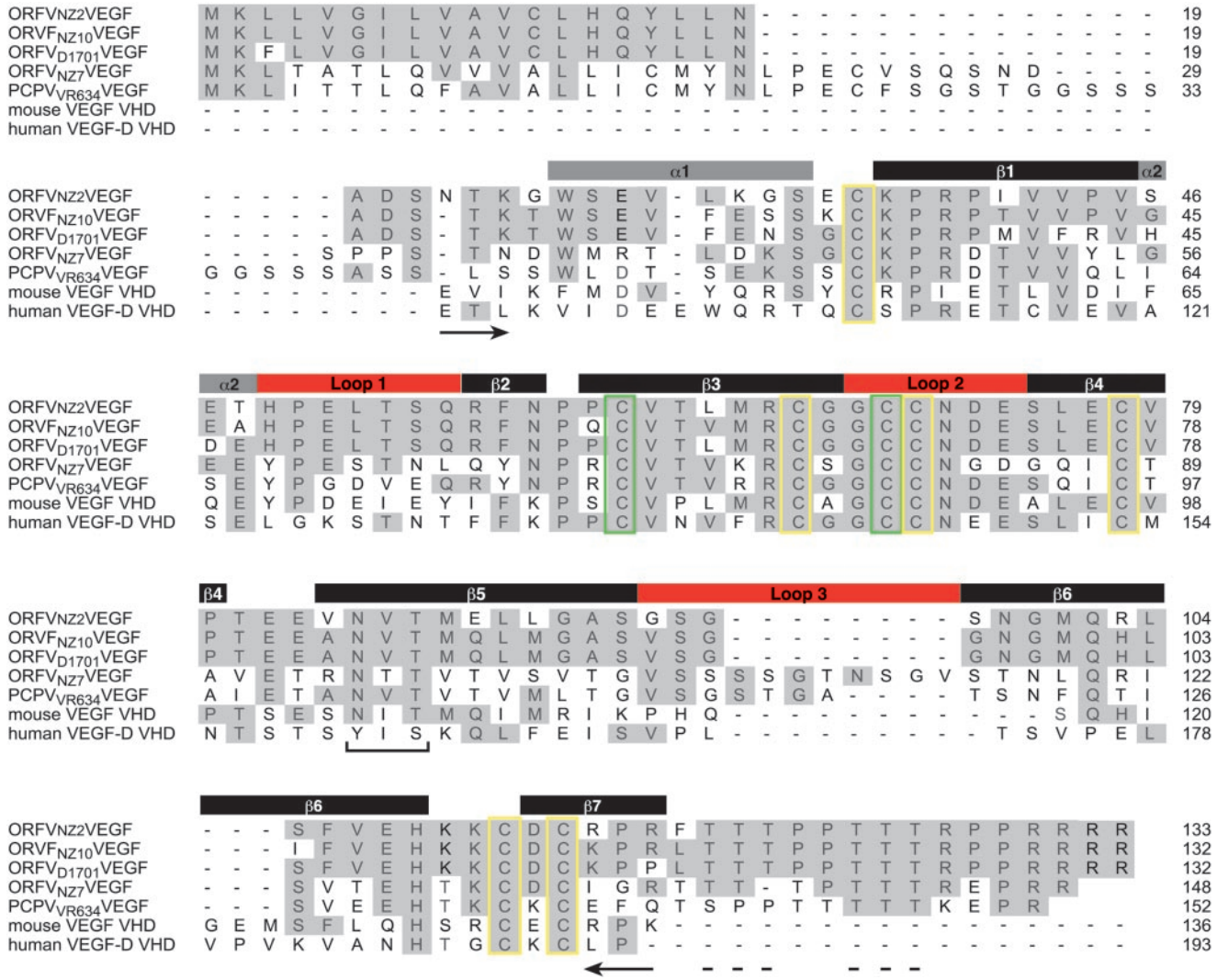

FIG. 1. **Comparison of viral VEGF variants and selected mammalian VEGFs by sequence analysis.** Alignment of the amino acid sequences of the viral VEGF variants with mouse VEGF-A and human VEGF-D in the region of the VHD. Residues matching the consensus of the alignment of the viral VEGFs are *shaded*. Secondary structural elements of the VHD are indicated and *numbered* above the alignment by *gray*, *black*, and *red boxes* representing α-helices, β-strands, and variable loops, respectively. The conserved cysteine residues that form intramolecular- and intermolecular-disulphide bonds within the cystine knot motif are *boxed* in *yellow* and *green*, respectively. The potential sites of *N*- and *O*-linked glycosylation conserved by the viral VEGFs are indicated by a *bracket* and *dashed line*, respectively below the alignments. The borders of the VHD are indicated by *arrows* below the alignment.

permeability. ORFV$_{D1701}$VEGF showed greater potency than ORFV$_{NZ2}$VEGF and PCPV$_{VR634}$VEGF, which in turn were more potent than ORFV$_{NZ10}$VEGF and ORFV$_{NZ7}$VEGF. These results clearly demonstrate that the viral VEGFs vary in their abilities to induce vascular permeability in the guinea pig. In addition there is no significant correlation ($p \geq 0.05$) between the mitogenic potencies of the viral VEGFs and their abilities to induce vascular permeability.

Viral VEGF Variants Induce Angiogenesis in Vivo—The abilities of the viral VEGF variants to induce angiogenesis *in vivo* were tested in sheep, the natural host of *Orf virus*. Sheep were injected intradermally with equal concentrations of mVEGF$_{164}$, hVEGF-DΔNΔC, and each viral VEGF in quadruplicate. Also included, as negative controls, were FLAG-tagged ovine IL-10, orf virus IL-10, PBS, and a mock elution sample. Each site was boosted after 72 h with an equal dose of the same factor to mimic the continued exposure that would occur in a viral infection. After 9 days biopsies were taken from each site and the adjacent untreated skin then analyzed histologically. Representative sections from normal and treated skin are shown in Fig. 3*A*. The extent of dermal vascularization was analyzed by determining the areal fraction of dermis reacting with the anti-human von Willebrand factor antibody, which is a specific marker for endothelial cells. Each of the growth factors was able to induce a significant increase ($p \leq 0.05$) in the number of endothelial cells in the dermis compared with untreated skin (Fig. 3*B*). FLAG-tagged ovine and orf virus IL-10, PBS, and the mock elution, however, showed no significant increase ($p \geq 0.05$). Statistical analyses revealed no significant difference in potency between mVEGF$_{164}$ and ORFV$_{NZ2}$VEGF, ORFV$_{NZ10}$VEGF, or ORFV$_{D1701}$VEGF. ORFV$_{NZ7}$VEGF, however, was significantly more potent than mVEGF$_{164}$, whereas PCPV$_{VR634}$VEGF and hVEGF-DΔNΔC were less potent. These results clearly demonstrate that all the viral VEGF variants are effective mitogens for sheep endothelial cells, with only the VEGF derived from *Pseudocowpox virus* exhibiting a potency lower than mVEGF$_{164}$.

Viral VEGF Variants Bind VEGFR-2—To determine whether the variation in primary amino acid sequence among the different viral VEGFs translated to differing receptor binding profiles we examined their abilities to bind the mammalian tyrosine kinase receptors, VEGFR-1, VEGFR-2 or VEGFR-3.

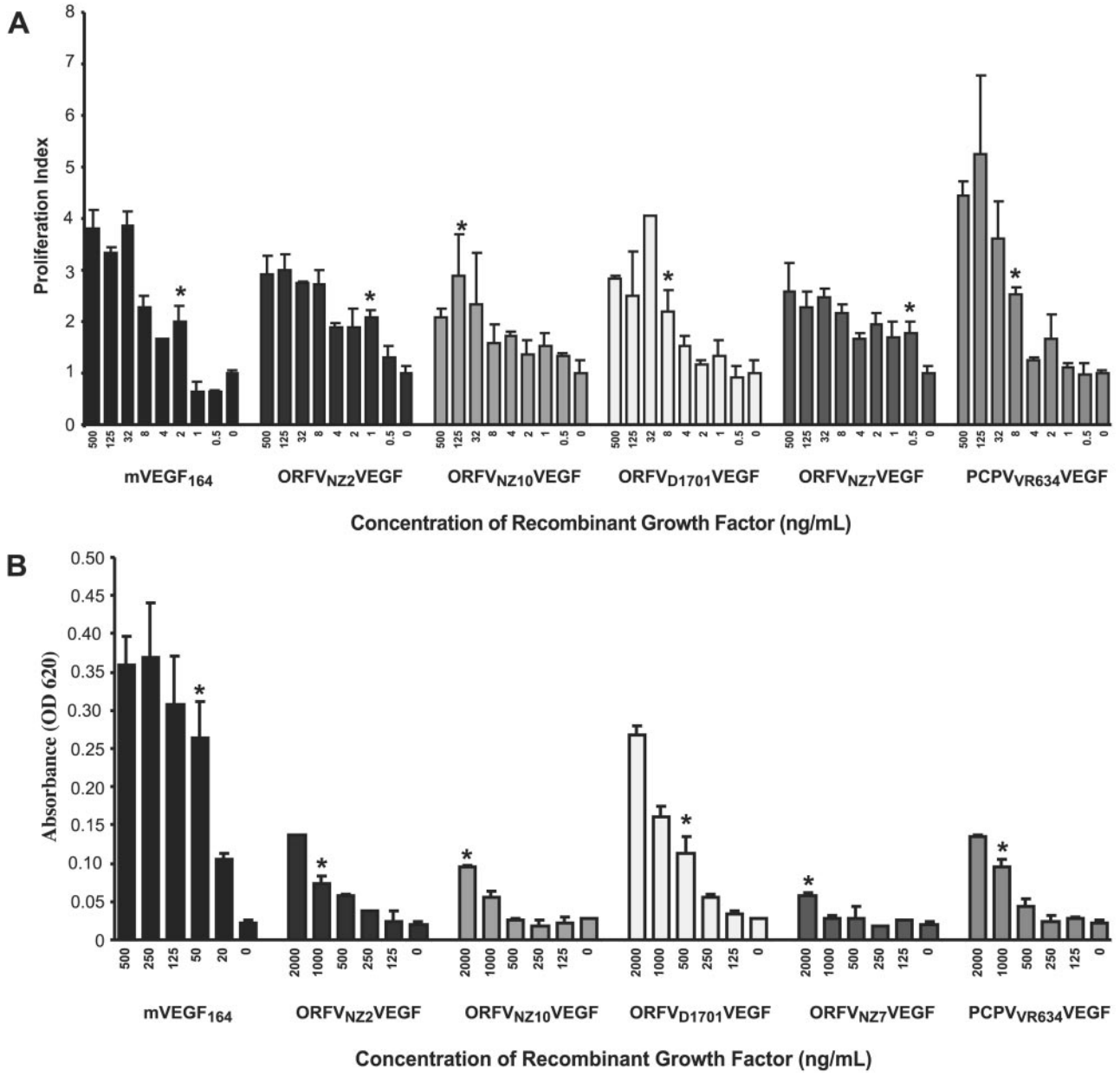

FIG. 2. **Evaluation of the biological activities of the viral VEGF variants.** *A*, the mitogenic activity of the mammalian and viral VEGF variants was tested in a HMVEC mitogenic assay. HMVECs (10^4) were incubated with dilutions of purified mammalian and viral VEGF variants, or medium alone for 72 h at 37 °C. After incubation, cellular growth was quantitated by counting of cells. Values are the mean of four replicates ± S.D. and are expressed as a proliferation index, which refers to the ratio of the number of cells in each supplemented sample compared with that from medium alone. The results shown are representative of three experiments. The lowest dose of each sample that induced a significant increase in proliferation, over background, is indicated by an *asterisk* ($p \leq 0.05$). *B*, the ability of the mammalian and viral VEGF variants to induce vascular permeability was tested in the Miles assay. Dilutions of purified mammalian and viral VEGF variants and standard controls of $mVEGF_{164}$ and PBS alone were injected intradermally into guinea pigs that had Evans blue dye circulating in their blood streams. The patch of skin at the site of each injection was excised and the dye was extracted from the skin with formamide and the absorbance at 620 nm was recorded. OD values were normalized across the animals using the ratio of the standard controls, and are expressed as the mean of two replicates ± S.D., and are representative of three experiments. The lowest concentration of each sample that showed a significant increase in absorbance over background is indicated by an *asterisk* ($p \leq 0.05$).

The viral VEGFs along with $mVEGF_{164}$ and hVEGF-DΔNΔC were tested for their capacity to bind to the soluble, dimerized Ig fusion proteins containing the extracellular domains of VEGFR-1, VEGFR-2, and VEGFR-3 (21, 36).

Labeled VEGF proteins that bound to the fusion proteins were analyzed using SDS-PAGE. Quantitation of the precipitated bands showed that all the viral VEGFs bound both human VEGFR-2 and murine VEGFR-2 less avidly than did $mVEGF_{164}$ (Fig. 4*A*). In the case of human VEGFR-2, all the viral VEGF variants showed a uniform 2.5-fold reduction in the level of binding relative to mouse $VEGF_{164}$, similar to that of hVEGF-DΔNΔC. In the case of mouse VEGFR-2, there was also evidence of differences between the viral VEGFs. The VEGFR-1-Ig fusion protein bound $mVEGF_{164}$ but not hVEGF-DΔNΔC or any of the viral VEGFs (Fig. 4*A*). The VEGFR-3-Ig fusion protein, however, bound hVEGF-DΔNΔC but not $mVEGF_{164}$ or any of the viral VEGFs (Fig. 4*A*). These results clearly demonstrate that all of the viral VEGF variants share a receptor binding profile, binding to the extracellular domain of VEGFR-2 but not those of VEGFR-1 or VEGFR-3.

Viral VEGF Variants Differ in Their Ability to Bind and Cross-link VEGFR-2—The interactions between the viral

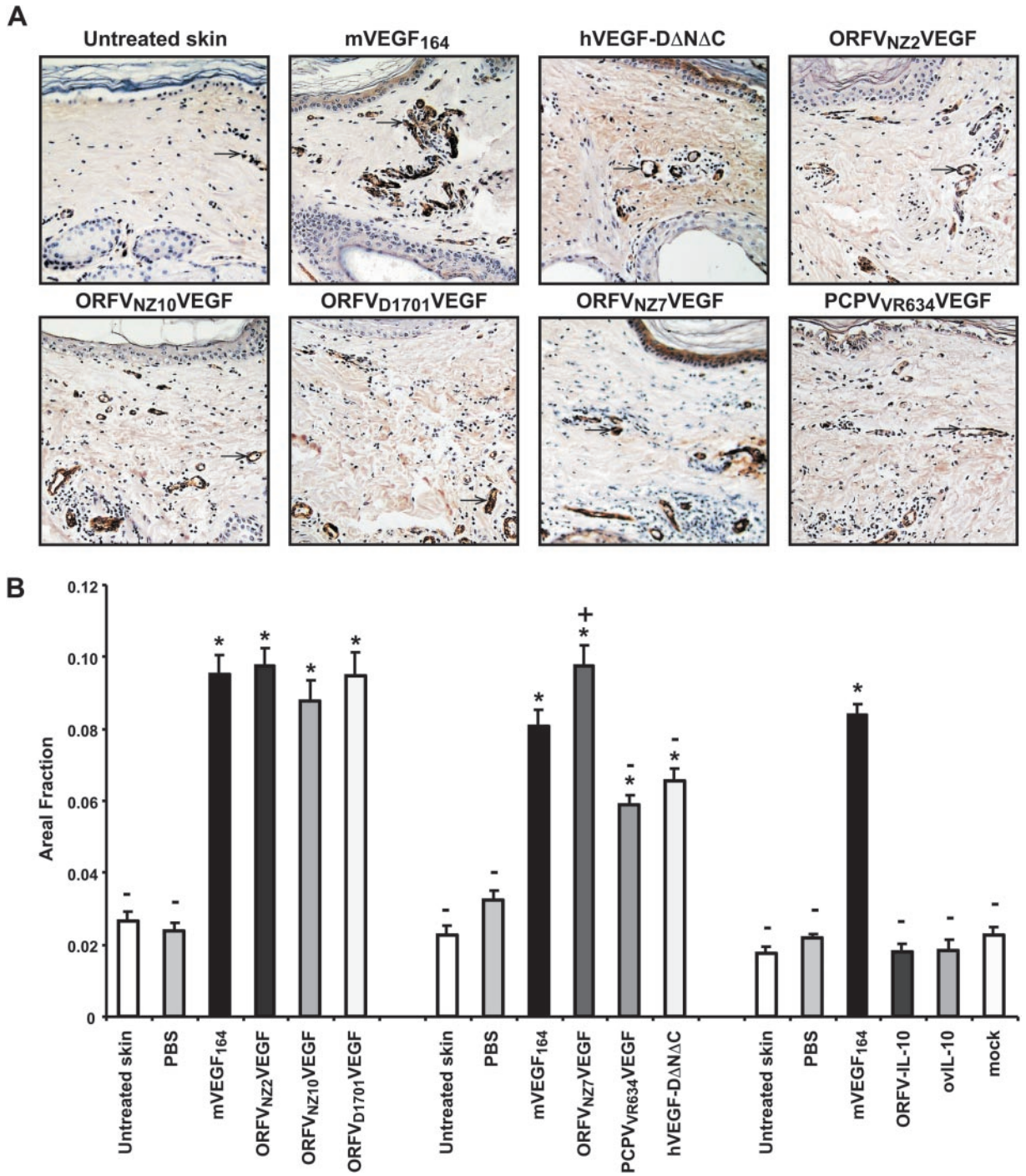

FIG. 3. **Evaluation of the angiogenic response induced *in vivo* by viral VEGF variants.** *A*, histological comparison of the angiogenic response induced in sheep skin by representative mammalian and viral VEGF variants compared with untreated skin. 2 μg of purified mammalian and viral VEGF variants and controls, including FLAG-tagged ovine and *orf virus* IL-10, PBS, and a mock elution sample were injected intradermally into sheep skin and boosted with a second injection after 72 h. The skin around each injection site and normal skin was biopsied after 9 days, and the vascularization was assessed using anti-human von Willebrand factor antibody. *Arrows* indicate representative blood vessels highlighted by the antibody staining. *B*, the extent of dermal vascularization was quantified by determining the areal fraction of dermis reacting with the anti-human von Willebrand factor antibody from three equidistant sections as outlined under "Experimental Procedures." Values are expressed as the mean areal fraction ± S.E. The areal fraction values that are significantly above that of untreated skin are indicated by an *asterisk* ($p \leq 0.05$). The areal fraction values that are significantly above that of $mVEGF_{164}$ are indicated by a + and those significantly below by a − ($p \leq 0.05$).

VEGFs and the receptors, VEGFR-2 and VEGFR-3, were tested further in bioassays that detect receptor binding and cross-linking at the cell surface. These specific assays made use of Ba/F3 cells expressing chimeric receptors consisting of either the extracellular domain of VEGFR-2 or VEGFR-3 and the transmembrane and cytoplasmic domains of erythropoietin receptor.

With the VEGFR-2 bioassay cell line, in the presence of heparin, $mVEGF_{164}$, hVEGF-DΔNΔC and each of the viral VEGFs were able to induce significant increases ($p \leq 0.05$) in DNA synthesis compared with medium that contained no added growth factors (Fig. 4*B*). Statistical analyses revealed that at the highest concentration tested (250 ng/ml), $mVEGF_{164}$ and $ORFV_{D1701}VEGF$ were significantly more po-

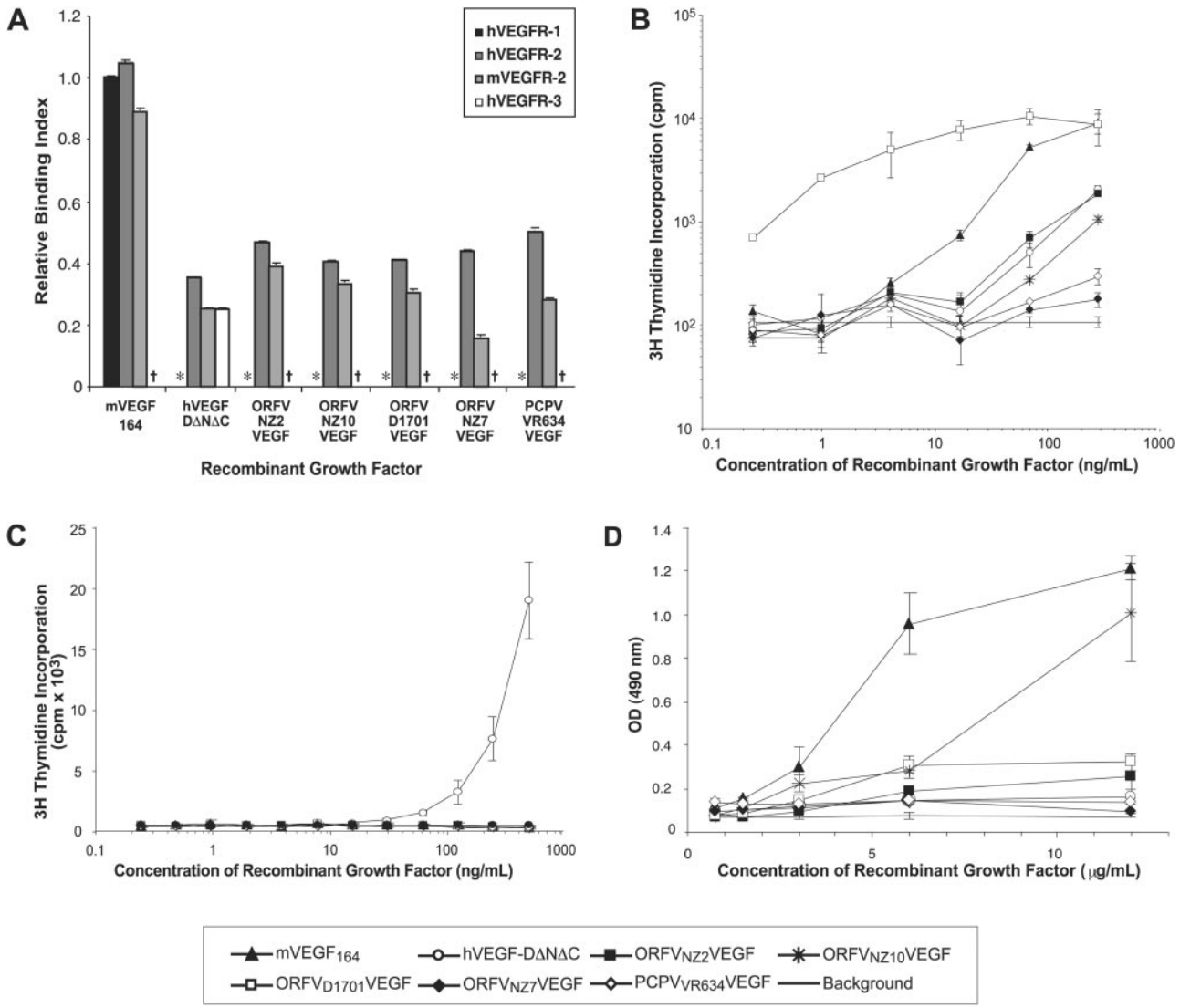

FIG. 4. **Receptor-binding specificity of the viral VEGF variants.** *A*, mammalian and viral VEGF variants were assessed for binding to human (*h*) VEGFR-1, VEGFR-2, and VEGFR-3 and murine (*m*) VEGFR-2 by immunoprecipitation of metabolically labeled, FLAG-tagged VEGFs using the soluble VEGFR-Ig fusion proteins as described under "Experimental Procedures." Washed precipitates were eluted and analyzed by SDS-PAGE under reducing conditions. Precipitated proteins were visualized using phosphorimaging analysis and quantified using the program Quantity One. Levels of binding of the ligands to the VEGFR-Ig fusion proteins were expressed as a relative binding index ± S.E., which is the ratio of the amount of labeled VEGF precipitated by a receptor divided by the total amount available to be precipitated as measured in a separate reaction between the labeled, FLAG-tagged VEGFs and anti-FLAG-agarose. An *asterisk* indicates that binding to VEGFR-1 was not detected and a *cross* indicates that binding to VEGFR-3 was not detected. *B*, the ability of the mammalian and viral VEGF variants to bind and cross-link mouse VEGFR-2 was tested using an mVEGFR-2-specific bioassay cell-line. Bioassay cells were washed and resuspended in dilutions of purified mammalian and viral VEGF variants, or medium alone, for 48 h at 37 °C, in the presence of heparin. DNA synthesis was quantitated by [^{3}H]thymidine incorporation and β-counting. Values are expressed as the mean of two replicates ± S.D. and are representative of four experiments. *Symbols* representing each growth factor in *B*, *C*, and *D* are indicated in the *panel below*. *C*, the ability of the mammalian and viral VEGF variants to bind and cross-link human VEGFR-3 was tested using an hVEGFR-3-specific bioassay cell-line (as described in *B*). Values are expressed as the mean of two replicates ± S.D. and are representative of three experiments. *D*, the ability of the mammalian and viral VEGF variants to bind rat NP-1 was tested using an ELISA. Dilutions of purified FLAG-tagged mammalian and viral VEGF variants, or mock-purified protein (background) were added to plates coated with NP-1-Ig fusion protein. The amount of bound FLAG-tagged protein was measured using an anti-FLAG (M2) -horseradish peroxidase conjugate and *O*-phenylenediamine substrate. Values are expressed as the mean of two replicates ± S.E. and are representative of three experiments.

tent than $ORFV_{NZ2}VEGF$, $ORFV_{NZ10}VEGF$, and hVEGF-DΔNΔC, which in turn were significantly more potent than $ORFV_{NZ7}VEGF$ and $PCPV_{VR634}VEGF$. Surprisingly $ORFV_{D1701}$-VEGF was significantly more potent than all of the other factors, including $mVEGF_{164}$, at the lower range of concentrations (0.125–16 ng/ml). Although demonstrating similar abilities to bind the VEGFR-2-Ig fusion proteins, the viral VEGFs surprisingly varied significantly in their ability to bind and cross-link VEGFR-2 at the cell surface.

With the VEGFR-3 bioassay cell line, hVEGF-DΔNΔC was able to induce a significant increase in DNA synthesis from a concentration of 50 ng/ml (Fig. 4*C*). Consistent with their lack of binding to VEGFR-3, mouse $VEGF_{164}$ and each of the viral VEGFs were unable to induce DNA synthesis via this receptor.

Viral VEGF Variants Differ in Their Ability to Bind NP-1—To assess their interaction with the NP-1, the viral VEGFs along with $mVEGF_{164}$ and hVEGF-DΔNΔC were tested for their capacity to bind the soluble, dimerized Ig fusion protein containing the extracellular domains of NP-1 using an ELISA (Fig. 4*D*). Mouse $VEGF_{164}$, $ORFV_{NZ10}VEGF$, $ORFV_{NZ2}VEGF$, and $ORFV_{D1701}VEGF$ demonstrated significant levels of binding to NP-1 compared with mock-purified protein. Statistical

analyses revealed that $mVEGF_{164}$ and $ORFV_{NZ10}VEGF$ bound NP-1 more avidly than either $ORFV_{NZ2}VEGF$ or $ORFV_{D1701}$-VEGF. $ORFV_{NZ7}VEGF$, $PCPV_{VR634}VEGF$, and hVEGF-DΔNΔC were, however, unable to bind NP-1 at the concentrations tested. These results reveal that the viral VEGFs exhibit significant variation in their abilities to bind NP-1.

DISCUSSION

The extensive variation in amino acid sequence between individual viral VEGFs lead us to question if this variation was reflected in functional variations. We therefore undertook direct functional comparisons of a representative selection of parapoxvirus VEGF variants. Our data reveal significant variation in the activities of the viral VEGFs, specifically in their abilities to cross-link VEGFR-2, induce vascular permeability, and bind NP-1. In contrast, we show that the viral VEGFs are all mitogenic for human endothelial cells, and all are able to induce angiogenesis *in vivo* with potencies, in both assays, equivalent to that of $mVEGF_{164}$.

The mitogenic activities of the viral VEGFS are achieved despite their reduced abilities, compared with $mVEGF_{164}$, to bind VEGFR-2. These observations are in contrast with studies of cellular members of the VEGF family, which have shown that the mitogenic potencies of, for example, VEGF-C and VEGF-D are reflected in their reduced affinity for VEGFR-2 (9, 10, 41). Consistent with this we have shown here that VEGF-DΔNΔC has a reduced binding affinity for VEGFR-2, equivalent to the viral VEGFs, but unlike the viral VEGFs has a parallel reduction in its ability to induce angiogenesis in sheep skin.

There are several possible mechanisms by which the viral VEGFs might induce levels of biological activity comparable with that of VEGF-A, despite their lower receptor-binding abilities and their varying receptor cross-linking abilities. The binding affinity of the viral VEGFs for VEGFR-2 could be enhanced through their interaction with other cell surface molecules such as neuropilin. However, the varying and generally reduced levels of binding of the viral VEGFs to NP-1 suggest that, in contrast to VEGF-A, NP-1 is not involved in stabilizing the binding of the viral VEGFs to VEGFR-2, at least in the context of mitogenic signaling. Alternatively, the viral VEGFs may utilize different signaling strategies. For example, VEGF-C, despite a reduced affinity for VEGFR-2 induces more sustained signaling via this receptor than does VEGF-A (38). Further examples are provided by the epidermal growth factors of several poxviruses, which employ a range of novel receptor activation strategies and thereby are as mitogenic as their cellular counterparts despite lower receptor-binding affinities (42).

In contrast to their effective and uniform mitogenic activity, each of the viral VEGFs induced substantially less vascular permeability than was seen with VEGF-A and their potencies in this assay varied between individual factors. Interestingly $ORFV_{D1701}VEGF$ was significantly more potent than the other viral VEGFs in both the assay of vascular permeability and the bioassay detecting the binding and cross-linking of VEGFR-2. Statistical analysis confirmed there was a significant correlation ($p \leq 0.05$) between the viral VEGFs' abilities to induce vascular permeability and to bind and cross-link VEGFR-2. The molecular mechanisms by which VEGF-A induces vascular permeability, in particular the cell surface receptor(s) responsible, have not been fully characterized (43), but our data are consistent with recent studies that suggested a role for VEGFR-2 in vascular permeability (44–47). The lack of correlation between the viral VEGFs' mitogenic and vascular permeability activities suggests that vascular permeability and mitogenesis are mediated through different pathways, although both may be induced by the dimerization of VEGFR-2 at the cell surface.

Statistical analysis revealed a surprising correlation ($p \leq 0.05$) between the ability to induce vascular permeability and NP-1 binding. In addition we have shown that VEGF-D, which fails to induce significant levels of vascular permeability (33), binds VEGFR-2 but not NP-1. On the other hand, PlGF and VEGF-B also fail to induce significant levels of vascular permeability, but bind NP-1 and not VEGFR-2 (19, 48). These data are suggestive of a role of NP-1 in mediating permeability in association with the dimerization of VEGFR-2.

It is interesting to note that when assays were conducted using assay systems derived from species that are natural hosts of *Orf virus* (sheep and human), the viral VEGFs were essentially equivalent to each other in receptor specificity and biological activity. However, in assays conducted using non-host species (mouse, rat, and guinea pig) the viral VEGFs varied in activity. There was, however, very little evidence of differences in the abilities of the viral VEGFs to bind soluble VEGFR-2, from host and non-host species. Differences that were observed, although warranting further investigation, failed to account for the extent of the variation between the viral VEGFs in NP-1 binding, the cross-linking of VEGFR-2, and the induction of vascular permeability.

The establishment of comparative functional data for the viral VEGF variants allowed us to look for correlations between function and sequence or structure. The predicted structures of the viral VEGFs are generally similar to that of VEGF-A conserving the locations of the anti-parallel β-sheets and the cysteine residues that form the intra- and inter-chain disulphide bonds responsible for cystine knot formation (Fig. 5). Within the VHDs of the viral VEGFs, only 32% of the amino acids are conserved in all five of the variants. This variation is illustrated in Fig. 5, which shows the paucity of amino acids conserved between, for example, $ORFV_{NZ7}VEGF$ and $PCPV_{VR634}VEGF$. Although the viral VEGFs retain the three loop regions involved in the binding of VEGF-A to VEGFR-2, they conserve very few of the specific residues identified by mutational analyses and alanine substitutions as being required for VEGFR-2 recognition by VEGF-A (Fig. 5) (49–51). This might indicate that alternative motifs are able to effectively activate VEGFR-2 signaling or that the general structure conserved by the viral VEGFs is sufficient to activate VEGFR-2 and that specific residues are of lesser importance.

The most striking functional variations seen between the viral VEGFs were in the assays of VEGFR-2 cross-linking and of NP-1 binding. $ORFV_{D1701}VEGF$ was particularly potent in the bioassay of binding and cross-linking VEGFR-2 (Fig. 4*B*) but was no more potent than the other VEGFs when assayed for binding to a preformed dimer of the same receptor (Fig. 4*A*). Only 6 amino acids of $ORFV_{D1701}VEGF$ (Asn^{32}, Met^{40}, Phe^{42}, Arg^{43}, His^{45}, and Asp^{46}) are unique to this VEGF and not present in other factors including the closely related factors, $ORFV_{NZ2}VEGF$ and $ORFV_{NZ10}VEGF$. These residues, except for Asn^{32}, are clustered on the membrane-facing side of the dimer where they are likely to be able to interact with domain 3 of VEGFR-2 (52, 53). This is consistent with a model in which interaction between VEGF and domain 3 of the receptor promotes receptor dimerization by bringing the fourth domains of two monomers into close proximity. $ORFV_{D1701}VEGF$ was also the most potent viral VEGF in the induction of vascular permeability, and we observed a correlation between the viral VEGFs' abilities to induce vascular permeability and to bind and cross-link VEGFR-2. The fact that both assays were conducted using rodents makes it tempting to speculate that an

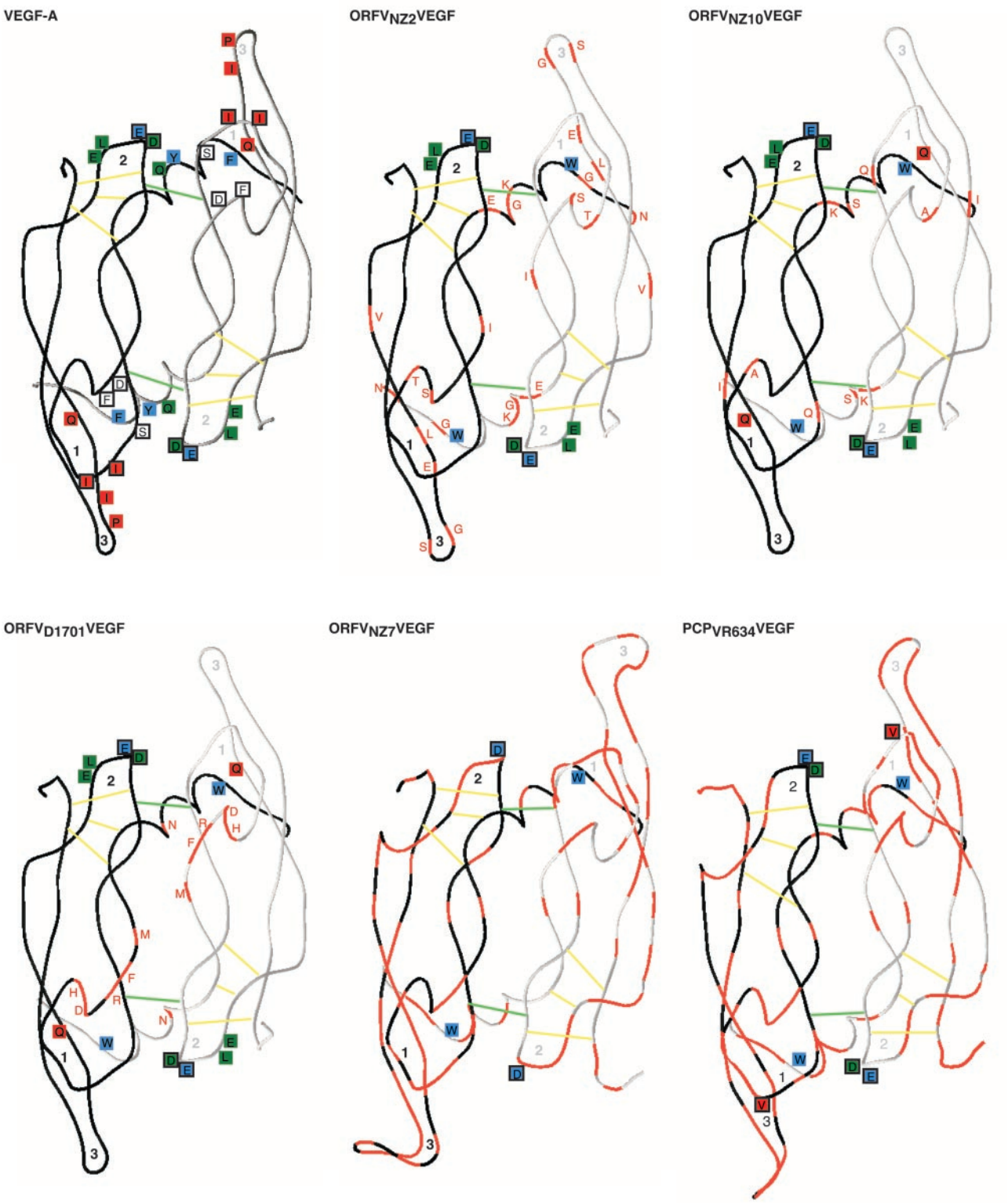

FIG. 5. **Representation of the structure of the VEGF-A dimer and the predicted structures of dimers of the viral VEGFs.** The sequences used in construction of the models were the VHDs listed in Fig. 1. The models were derived as described under "Experimental Procedures." One monomer of each dimer is shown in a *darker shade*. The conserved intramolecular- and intermolecular-disulphide bonds are shown in *yellow* and *green*, respectively. The variable loop regions are *numbered*. The locations of amino acids of VEGF-A predicted to be involved in receptor binding are marked. These residues are *shaded* and *colored* to indicate that they have been implicated in mediating the binding of VEGF-A to VEGFR-1 (*green*), VEGFR-2 (*red*), or both receptors (*blue*). Residues of VEGF-A forming a groove implicated in VEGFR-1 binding are *boxed* (*black*). Where these residues are conserved in the viral VEGFs they are *colored* in the same manner. On the viral models, residues that differ from the consensus of the alignment of the viral VEGFs (Fig. 1) are *highlighted* (*red*) and are labeled on the NZ2-like VEGFs.

enhanced ability to interact with VEGFR-2 domain 3 of rodents might be linked to both results. Interestingly, the majority of the sequence differences between the ligand-binding domains of human and mouse VEGFR-2 occur in domain 3. The sequence of guinea pig VEGFR-2 has not been reported.

The ability of the NZ2-like viral VEGFs to bind NP-1 is

surprising given their lack of conservation of the heparin-binding domain implicated in the binding of VEGF-A, VEGF-B, and PlGF to NP-1 (19, 48, 54). Indeed, these are the only VEGF family members reported to interact with NP-1 independently of heparin binding. The viral VEGFs differed in their ability to bind NP-1, with only $ORFV_{NZ10}$VEGF binding at levels comparable with $mVEGF_{164}$. The amino acids unique to $ORFV_{NZ10}$VEGF and which are presumed to be responsible for this enhanced binding to NP-1 are dispersed through the VHD (Fig. 1), but structural modeling shows them to be clustered in two sites (Fig. 5). One site (Ser^{32} and Lys^{34}) lies between the monomers in the region of the VEGFR-binding domain of the dimer. The other site (Ala^{47} and Ile^{104}) is on the side of the dimer in the region of the juxtaposition of α-helix 2 and β-strand 6. Neither site has previously been linked to NP binding, and they appear to represent at least one novel site of interaction between a VEGF family member and NP-1.

All the viral VEGFs differ from VEGF-A in their lack of recognition of VEGFR-1, despite having several of the amino acids thought to be important in binding this receptor (Fig. 5). Structural determinations have revealed a groove at each end of the VEGF-A dimer and it has been postulated that these are involved in the recognition of VEGFR-1 (52, 53). Residues forming this groove in VEGF-A are indicated in Fig. 5. Structural modeling predicts that the presence in the viral VEGFs of an Arg in place of Ser^{50} and/or Ile^{46} has the effect blocking this groove (26). Similar predictions can be made for VEGF-C and VEGF-D, whereas in the case of VEGF-B and PlGF, the groove appears to be open. These modeling predictions of the status of the groove correlate with the ability to recognize VEGFR-1, and we suggest that the absence of an effective groove inhibits the binding of the viral VEGFs to VEGFR-1. A corollary of this working model is that effective recognition of VEGFR-2 is not dependent on the groove-linker interaction. Each viral VEGF contains a Gly/Ser-rich insertion in the loop 3 region, which is most pronounced in $ORFV_{NZ7}$VEGF and $PCPV_{VR634}$VEGF. In addition the viral VEGFs conserve a unique Pro/Thr-rich sequence, encoding potential *O*-linked glycosylation sites, at their C termini. Both of these structural elements might also play a role of blocking binding to VEGFR-1.

The functional and evolutionary significance of the extensive amino acid sequence variation shown by the viral VEGFs remains an intriguing question. The retention of uniform angiogenic abilities despite the extreme sequence variation indicates that the stimulation of angiogenesis is an important viral function and that the sequence variation does not arise as a result of the gene encoding a redundant activity. Each of the viral VEGFs also shared the inability to bind VEGFR-1. It has been proposed that VEGFR-1 may act as a negative regulator of angiogenesis, sequestering VEGF molecules until a threshold level of protein is reached at which point any additional VEGF binds and activates VEGFR-2 (14). The absence of binding to VEGFR-1 could therefore increase the bioavailability of the viral VEGFs to the main mitogenic receptor, VEGFR-2. VEGFR-1 also appears to play a role in leukocyte migration and the maturation of dendritic cells (55–58). As these immune cells are important regulators of anti-viral responses, it would seem beneficial for a viral VEGF to avoid activating these responses via VEGFR-1. These observations suggest that the sequence differences between the viral VEGFs and VEGF-A may result from selection pressures against VEGFR-1 binding. On the other hand, the extensive variation between the viral VEGFs may demonstrate the variation that can occur when the constraints of VEGFR-1 binding (and perhaps NP-1 binding) are removed. The same variation also demonstrates the degree of sequence variability that can be tolerated while maintaining the ability to activate VEGFR-2. Given the complexity of the regulatory systems involved in vasculature formation (reviewed in Ref. 59), this tolerance of variation is unexpected.

Acknowledgments—We thank C. MacFarlane and M. Halford for supplying expression vectors and Y. Gunji and K. Pajusola for supplying plasmid constructs encoding VEGFR-Ig fusion proteins.

REFERENCES

1. Risau, W. (1997) *Nature* **386,** 671–674
2. Robinson, C. J., and Stringer, S. E. (2001) *J. Cell Sci.* **114,** 853–865
3. Stacker, S. A., and Achen, M. G. (1999) *Growth Factors* **17,** 1–11
4. Ferrara, N., and Henzel, W. J. (1989) *Biochem. Biophys. Res. Commun.* **161,** 851–858
5. Leung, D. W., Cachianes, G., Kuang, W. J., Goeddel, D. V., and Ferrara, N. (1989) *Science* **246,** 1306–1309
6. Senger, D. R., Galli, S. J., Dvorak, A. M., Perruzzi, C. A., Harvey, V. S., and Dvorak, H. F. (1983) *Science* **219,** 983–985
7. Maglione, D., Guerriero, V., Viglietto, G., Delli-Bovi, P., and Persico, M. G. (1991) *Proc. Natl. Acad. Sci. U. S. A.* **88,** 9267–9271
8. Olofsson, B., Pajusola, K., Kaipainen, A., von Euler, G., Joukov, V., Saksela, O., Orpana, A., Pettersson, R. F., Alitalo, K., and Eriksson, U. (1996) *Proc. Natl. Acad. Sci. U. S. A.* **93,** 2576–2581
9. Joukov, V., Pajusola, K., Kaipainen, A., Chilov, D., Lahtinen, I., Kukk, E., Saksela, O., Kalkkinen, N., and Alitalo, K. (1996) *EMBO J.* **15,** 1751
10. Achen, M. G., Jeltsch, M., Kukk, E., Makinen, T., Vitali, A., Wilks, A. F., Alitalo, K., and Stacker, S. A. (1998) *Proc. Natl. Acad. Sci. U. S. A.* **95,** 548–553
11. McDonald, N. Q., and Hendrickson, W. A. (1993) *Cell* **73,** 421–424
12. de Vries, C., Escobedo, J. A., Ueno, H., Houck, K., Ferrara, N., and Williams, L. T. (1992) *Science* **255,** 989–991
13. Quinn, T. P., Peters, K. G., De Vries, C., Ferrara, N., and Williams, L. T. (1993) *Proc. Natl. Acad. Sci. U. S. A.* **90,** 7533–7537
14. Shibuya, M. (2001) *Int. J. Biochem. Cell Biol.* **33,** 409–420
15. Taipale, J., Makinen, T., Arighi, E., Kukk, E., Karkkainen, M., and Alitalo, K. (1999) *Curr. Top. Microbiol. Immunol.* **237,** 85–96
16. Stacker, S. A., Caesar, C., Baldwin, M. E., Thornton, G. E., Williams, R. A., Prevo, R., Jackson, D. G., Nishikawa, S., Kubo, H., and Achen, M. G. (2001) *Nat. Med.* **7,** 186–191
17. Park, J. E., Chen, H. H., Winer, J., Houck, K. A., and Ferrara, N. (1994) *J. Biol. Chem.* **269,** 25646–25654
18. Olofsson, B., Korpelainen, E., Pepper, M. S., Mandriota, S. J., Aase, K., Kumar, V., Gunji, Y., Jeltsch, M. M., Shibuya, M., Alitalo, K., and Eriksson, U. (1998) *Proc. Natl. Acad. Sci. U. S. A.* **95,** 11709–11714
19. Migdal, M., Huppertz, B., Tessler, S., Comforti, A., Shibuya, M., Reich, R., Baumann, H., and Neufeld, G. (1998) *J. Biol. Chem.* **273,** 22272–22278
20. Soker, S., Takashima, S., Miao, H. Q., Neufeld, G., and Klagsbrun, M. (1998) *Cell* **92,** 735–745
21. Wise, L. M., Veikkola, T., Mercer, A. A., Savory, L. J., Fleming, S. B., Caesar, C., Vitali, A., Makinen, T., Alitalo, K., and Stacker, S. A. (1999) *Proc. Natl. Acad. Sci. U. S. A.* **96,** 3071–3076
22. Fuh, G., Garcia, K. C., and de Vos, A. M. (2000) *J. Biol. Chem.* **275,** 26690–26695
23. Lyttle, D. J., Fraser, K. M., Fleming, S. B., Mercer, A. A., and Robinson, A. J. (1994) *J. Virol.* **68,** 84–92
24. Ogawa, S., Oku, A., Sawano, A., Yamaguchi, S., Yazaki, Y., and Shibuya, M. (1998) *J. Biol. Chem.* **273,** 31273–31282
25. Meyer, M., Clauss, M., Lepple-Wienhues, A., Waltenberger, J., Augustin, H. G., Ziche, M., Lanz, C., Buttner, M., Rziha, H. J., and Dehio, C. (1999) *EMBO J.* **18,** 363–374
26. Mercer, A. A., Wise, L. M., Scagliarini, A., McInnes, C. J., Buettner, M., Rhiza, H. J., McCaughan, C. A., Fleming, S. B., Ueda, N., and Nettleton, P. F. (2002) *J. Gen. Virol.* **83,** 2845–2855
27. Ueda, N., Wise, L. M., Stacker, S. A., Fleming, S. B., and Mercer, A. A. (2003) *Virology* **305,** 298–309
28. Haig, D. M., and Mercer, A. A. (1998) *Vet. Res.* **29,** 311–326
29. Mercer, A., Fleming, S., Robinson, A., Nettleton, P., and Reid, H. (1997) *Arch. Virol. Suppl.* **13,** 25–34
30. Groves, R. W., Wilson-Jones, E., and MacDonald, D. M. (1991) *J. Am. Acad. Dermatol.* **25,** 706–711
31. Savory, L. J., Stacker, S. A., Fleming, S. B., Niven, B. E., and Mercer, A. A. (2000) *J. Virol.* **74,** 10699–10706
32. Mizushima, S., and Nagata, S. (1990) *Nucleic Acids Res.* **18,** 5322
33. Stacker, S. A., Vitali, A., Caesar, C., Domagala, T., Groenen, L. C., Nice, E., Achen, M. G., and Wilks, A. F. (1999) *J. Biol. Chem.* **274,** 34884–34892
34. Evans, M. J., Hartman, S. L., Wolff, D. W., Rollins, S. A., and Squinto, S. P. (1995) *J. Immunol. Methods* **184,** 123–138
35. Miles, A. A., and Miles, E. M. (1952) *J. Physiol. (Lond.)* **118,** 228–257
36. Achen, M. G., Roufail, S., Domagala, T., Catimel, B., Nice, E. C., Geleick, D. M., Murphy, R., Scott, A. M., Caesar, C., Makinen, T., Alitalo, K., and Stacker, S. A. (2000) *Eur. J. Biochem.* **267,** 2505–2515
37. Baldwin, M. E., Catimel, B., Nice, E. C., Roufail, S., Hall, N. E., Stenvers, K. L., Karkkainen, M. J., Alitalo, K., Stacker, S. A., and Achen, M. G. (2001) *J. Biol. Chem.* **276,** 19166–19171
38. Makinen, T., Veikkola, T., Mustjoki, S., Karpanen, T., Catimel, B., Nice, E. C., Wise, L., Mercer, A., Kowalski, H., Kerjaschki, D., Stacker, S. A., Achen, M. G., and Alitalo, K. (2001) *EMBO J.* **20,** 4762–4773
39. Guex, N., and Peitsch, M. C. (1997) *Electrophoresis* **18,** 2714–2723
40. Muller, Y. A., Christinger, H. W., Keyt, B. A., and de Vos, A. M. (1997) *Structure* **5,** 1325–1338
41. Lee, J., Gray, A., Yuan, J., Luoh, S. M., Avraham, H., and Wood, W. I. (1996)

Proc. Natl. Acad. Sci. U. S. A. **93,** 1988–1992
42. Tzahar, E., Moyer, J. D., Waterman, H., Barbacci, E. G., Bao, J., Levkowitz, G., Shelly, M., Strano, S., Pinkas-Kramarski, R., Pierce, J. H., Andrews, G. C., and Yarden, Y. (1998) *EMBO J.* **17,** 5948–5963
43. Dvorak, H. F., Brown, L. F., Detmar, M., and Dvorak, A. M. (1995) *Am. J. Pathol.* **146,** 1029–1039
44. Gille, H., Kowalski, J., Li, B., LeCouter, J., Moffat, B., Zioncheck, T. F., Pelletier, N., and Ferrara, N. (2001) *J. Biol. Chem.* **276,** 3222–3230
45. Joukov, V., Kumar, V., Sorsa, T., Arighi, E., Weich, H., Saksela, O., and Alitalo, K. (1998) *J. Biol. Chem.* **273,** 6599–6602
46. Feng, D., Nagy, J. A., Brekken, R. A., Pettersson, A., Manseau, E. J., Pyne, K., Mulligan, R., Thorpe, P. E., Dvorak, H. F., and Dvorak, A. M. (2000) *J. Histochem. Cytochem.* **48,** 545–556
47. Dvorak, A. M., and Feng, D. (2001) *J. Histochem. Cytochem.* **49,** 419–432
48. Makinen, T., Olofsson, B., Karpanen, T., Hellman, U., Soker, S., Klagsbrun, M., Eriksson, U., and Alitalo, K. (1999) *J. Biol. Chem.* **274,** 21217–21222
49. Muller, Y. A., Li, B., Christinger, H. W., Wells, J. A., Cunningham, B. C., and de Vos, A. M. (1997) *Proc. Natl. Acad. Sci. U. S. A.* **94,** 7192–7197
50. Li, B., Fuh, G., Meng, G., Xin, X., Gerritsen, M. E., Cunningham, B., and de Vos, A. M. (2000) *J. Biol. Chem.* **275,** 29823–29828
51. Keyt, B. A., Nguyen, H. V., Berleau, L. T., Duarte, C. M., Park, J., Chen, H., and Ferrara, N. (1996) *J. Biol. Chem.* **271,** 5638–5646
52. Iyer, S., Leonidas, D. D., Swaminathan, G. J., Maglione, D., Battisti, M., Tucci, M., Persico, M. G., and Acharya, K. R. (2001) *J. Biol. Chem.* **276,** 12153–12161
53. Wiesmann, C., Fuh, G., Christinger, H. W., Eigenbrot, C., Wells, J. A., and de Vos, A. M. (1997) *Cell* **91,** 695–704
54. Whitaker, G. B., Limberg, B. J., and Rosenbaum, J. S. (2001) *J. Biol. Chem.* **276,** 25520–25531
55. Detmar, M., Brown, L. F., Schon, M. P., Elicker, B. M., Velasco, P., Richard, L., Fukumura, D., Monsky, W., Claffey, K. P., and Jain, R. K. (1998) *J. Invest. Dermatol.* **111,** 1–6
56. Clauss, M., Weich, H., Breier, G., Knies, U., Rockl, W., Waltenberger, J., and Risau, W. (1996) *J. Biol. Chem.* **271,** 17629–17634
57. Gabrilovich, D. I., Chen, H. L., Girgis, K. R., Cunningham, H. T., Meny, G. M., Nadaf, S., Kavanaugh, D., and Carbone, D. P. (1996) *Nat. Med.* **2,** 1096–1103
58. Staquet, M. J., Godefroy, S., Jacquet, C., Viac, J., and Schmitt, D. (2001) *Arch. Dermatol. Res.* **293,** 26–28
59. Yancopoulos, G. D., Davis, S., Gale, N. W., Rudge, J. S., Wiegand, S. J., and Holash, J. (2000) *Nature* **407,** 242–248